

# The Outer-sphere Interactions in Ruthenium and Osmium Complexes

## I. Spectrophotometric and Voltammetric Studies on the Hydrogen Bonding Interactions of Bis(2,2'-bipyridine)(2-(2'-pyridyl)-benzimidazole)ruthenium(II) Cation and its Derivatives with Aromatic Nitrogen Heterocycles

MASA-AKI HAGA\* and AYAKO TSUNEMITSU

Department of Chemistry, Faculty of Education, Mie University, 1515 Kamihama, Tsu 514, Mie (Japan)

(Received January 30, 1989)

### Abstract

Spectrophotometric and electrochemical investigations have shown that the bis(2,2'-bipyridine)(2-(2'-pyridyl)-benzimidazole)ruthenium(II) cation and its derivatives interact with aromatic nitrogen heterocycles (N-heterocycles) through hydrogen bonding. The equilibrium constant for the hydrogen bonding was increased with increasing  $pK_a$  value of the N-heterocycles. The Ru(II/III) oxidation potential,  $E_{1/2}$ , was shifted cathodically by 200–400 mV due to the hydrogen bonding interaction. The magnitude of this potential shift shows the linear dependence on the base strength  $pK_a$  of the N-heterocycles. The hydrogen bonding interaction for the Ru(III) oxidation state was found to be much stronger than that for the Ru(II) state. We suggest the potential use of the present Ru–benzimidazole and –imidazole complexes as a spectrophotometric and electrochemical probe for examining the micro-environment in biopolymers.

### Introduction

Hydrogen bonding plays an important role in coordination chemistry. For example, the histidyl imidazole ligand in heme protein is hydrogen bonded to another group on the protein, which alters the chemical reactivity of the heme, particularly on the dioxygen binding property [1]. Several model systems involving simple imidazole complexes of ferrous and ferric porphyrins have been reported to mimic the influence of hydrogen bonding in native heme proteins. In these systems, the hydrogen bonding of the imidazole N–H moiety has been elucidated to affect the stability constants [2], ligand addition kinetics [1c], visible and Raman spectra [3] and redox potentials [4]. Furthermore, the hydrogen bonding has been shown to contribute to the stabilization of the specific outer-sphere

ion association between Co complexes and a variety of anions such as tartrate and sulfate in aqueous solutions [5]. This stabilization may be responsible for the optical resolution by using a resolving agent such as L-tartrate etc.

Recently, the importance of 'second-sphere' perturbation for the photochemistry of  $[\text{Co}(\text{CN})_6]^{3-}$  has been pointed out [6]. When  $[\text{Co}(\text{CN})_6]^{3-}$  gives rise to adducts with the polyammonium macrocycles 32- $\text{N}_8\text{H}_8^{8+}$  and 32- $\text{C}_9\text{N}_6\text{H}_6^{6+}$ , the quantum yields of the photoaquation reaction are noticeably smaller than that found for free  $[\text{Co}(\text{CN})_6]^{3-}$ . This result reflects an ionic-type interaction with a large contribution from hydrogen bonds between the peripheral nitrogen atoms of  $[\text{Co}(\text{CN})_6]^{3-}$  and the hydrogen atoms of the polyammonium cations. In addition, the solvent effect in the charge-transfer transition of the ruthenium–amine complexes has been interpreted by the hydrogen bonding type interaction involving electron-pair donation from a solvent molecule to the N–H bond [7]. Similarly, we have found that  $[\text{Ru}(\text{pby})_2(\text{BiBzImH}_2)]^{2+}$  exhibits strong solvent dependence on the oxidation potential. This solvent dependence has been explained by the hydrogen bonding interaction between the BiBzImH<sub>2</sub> ligand and the solvent [8].

In the present study, we examined the effect of hydrogen bonding on the properties of Ru–imidazole or –benzimidazole complexes. The tuning on the spectroscopic and electrochemical properties of  $[\text{Ru}(\text{bpy})_3]^{2+}$  and its derivatives is currently of interest because of the usefulness of  $[\text{Ru}(\text{bpy})_3]^{2+}$  as an attractive candidate for a photoredox sensitizer [9]. The possibility of the fine tuning on the properties of Ru complexes by outer-sphere interaction and that of the electrochemical and photochemical probes for biopolymers will be discussed for the present Ru–imidazole or –benzimidazole complexes. The imidazole and benzimidazole ligands and their abbreviations used here are shown in Fig. 1.

\* Author to whom correspondence should be addressed.

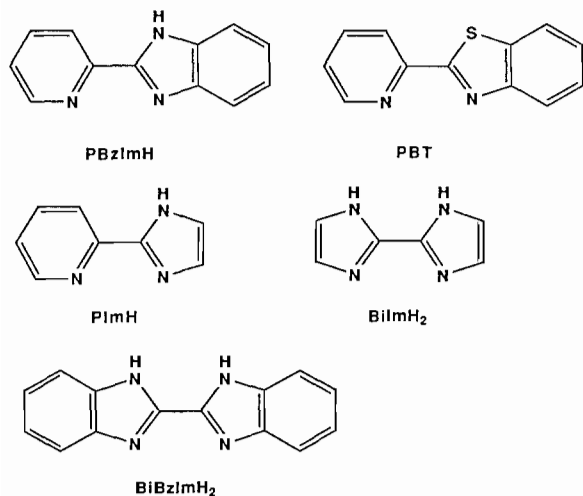


Fig. 1. The ligands and their abbreviations.

## Experimental

### Materials

Pyridine and 4-methylpyridine were purchased from Wako Pure Chemicals and purified by vacuum distillation. 4-t-Butylpyridine, 3-chloropyridine, 4-acetylpyridine and 1-methylimidazole, supplied by Aldrich, were distilled prior to use. 2-(2'-Pyridyl)-benzothiazole (PBT) [10] and tetrabutylammonium perchlorate (TBAP) [11] were prepared and purified by the literature method. Acetonitrile was distilled twice from calcium hydride. All other reagents were used as supplied.

### Preparation of Complexes

The complexes  $[\text{Ru}(\text{bpy})_2\text{L}](\text{ClO}_4)_2$  ( $\text{L} = \text{PImH}$ ,  $\text{PBzImH}$ ,  $\text{BiImH}_2$ , and  $\text{BiBzImH}_2$ ) were prepared as described previously [12]. The corresponding PBT complex was similarly prepared as follows.

The mixture of  $\text{Ru}(\text{bpy})_2\text{Cl}_2 \cdot \text{H}_2\text{O}$  (0.4 g, 0.8 mmol) and PBT (0.2 g, 1 mmol) was heated at reflux under nitrogen for 4 h in 1:1 vol./vol. ethanol-water (40 cm<sup>3</sup>), during which time the solution color changed from violet to red. To the resulting solution was added an excess of  $\text{NaClO}_4$  (1 g) in water (5 cm<sup>3</sup>). Upon cooling to 0 °C, the red crystals of  $[\text{Ru}(\text{bpy})_2(\text{PBT})](\text{ClO}_4)_2$  were deposited from the solution, collected by filtration, and recrystallized from methanol, 47% yield. *Anal. Calc.* for  $\text{C}_{32}\text{H}_{24}\text{N}_6\text{SO}_8\text{Cl}_2\text{Ru}$ : C, 46.61; H, 2.93; N, 10.19. *Found*: C, 46.64; H, 3.06; N, 10.25%.

### Physical Measurements

The electronic spectra were obtained on a Shimadzu UV-210 A double-beam spectrophotometer equipped with a 1 cm quartz cell, which was thermostated at  $25.0 \pm 0.2$  °C with a Yamato circulator

Model BF-41. Cyclic voltammetry was measured with a Hokuto Denko HA-301 potentiostat, a Hokuto Denko HF-201 function generator, and a Yokogawa x-y recorder Model 3086 as described before [12]. A silver wire served as a reference during the measurements. The potentials were calibrated with respect to an internal ferrocene/ferrocenium ( $\text{Fc}/\text{Fc}^+$ ) couple [13].

### The Evaluation of Equilibrium Constants for Hydrogen Bonding from UV Spectra

To obtain the equilibrium constants the spectral changes were measured in the  $\text{CH}_3\text{CN}$  solution of Ru complexes by adding an appropriate N-heterocycle. The concentration of Ru complex was kept constant at  $(1.5\text{--}8) \times 10^{-5}$  mol dm<sup>-3</sup>, and the concentration of N-heterocycles varied from 0 to 0.4 mol dm<sup>-3</sup>. Each titration was carried out at least two times. The absorbance data obtained from these titrations were analyzed by using the following equation [14]

$$\left(1 - \frac{d_0}{d}\right)/[D] = -K_1 + \left(\frac{\epsilon_c}{\epsilon_a}\right)\left(\frac{d_0}{d}\right)K_1 \quad (1)$$

where  $d$  and  $d_0$  are the absorbances at a fixed wavelength of interest with and without N-heterocycles, respectively, and  $[D]$  is the concentration of N-heterocycle.  $\epsilon_a$  and  $\epsilon_c$  are the molar extinction coefficients of a free Ru complex and a hydrogen bonded one, respectively. Plots between  $(1 - d_0/d)/[D]$  and  $(d_0/d)$  will give a straight line, and the equilibrium constants  $K_1$  can be evaluated as an intercept for the plots by using the least-squares method.

## Results and Discussion

### Equilibrium Constants between Ru Complexes and N-heterocycles from UV Spectra

Electronic spectra of  $[\text{Ru}(\text{bpy})_2(\text{PBzImH})]^{2+}$  in  $\text{CH}_3\text{CN}$  with varying amounts of 4-methylpyridine are shown in Fig. 2, in which the absorption maxima at 457 nm gradually decreased and new shoulder at 495 nm appeared on increasing the 4-methylpyridine concentration. The isosbestic points were observed at 407 and 478 nm. Similar spectral changes were obtained in the other systems of  $[\text{Ru}(\text{bpy})_2\text{L}]^{2+}$ -N-heterocycles ( $\text{L} = \text{PImH}$ ,  $\text{BiImH}_2$ , or  $\text{BiBzImH}_2$ ; N-heterocycle = 3-chloropyridine, 4-acetylpyridine, pyridine, 4-t-butylpyridine or 1-methylimidazole). On the other hand, the addition of a N-heterocycle to  $[\text{Ru}(\text{bpy})_3]^{2+}$  and  $[\text{Ru}(\text{bpy})_2(\text{PBT})]^{2+}$  in  $\text{CH}_3\text{CN}$  showed no spectral changes in the electronic spectra under the same conditions described above. No peripheral N-H hydrogen exists in the complexes  $[\text{Ru}(\text{bpy})_3]^{2+}$  and  $[\text{Ru}(\text{bpy})_2(\text{PBT})]^{2+}$ , which can be distinguished from the other complexes,

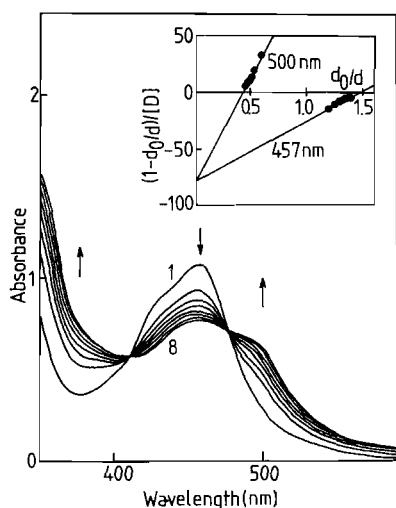


Fig. 2. Absorption spectra of  $8.50 \times 10^{-5} \text{ mol dm}^{-3}$   $[\text{Ru}(\text{bpy})_2(\text{PBzImH})]^{2+}$  in  $\text{CH}_3\text{CN}$  at  $25^\circ\text{C}$  with varying concentrations of 4-methylpyridine (Mepy): [Mepy] = (1) 0, (2)  $1.25 \times 10^{-2}$ , (3)  $2.49 \times 10^{-2}$ , (4)  $3.72 \times 10^{-2}$ , (5)  $4.95 \times 10^{-2}$ , (6)  $6.16 \times 10^{-2}$ , (7)  $7.37 \times 10^{-2}$ , (8)  $8.57 \times 10^{-2} \text{ mol dm}^{-3}$ . Plots of  $(1 - d_0/d)/[D]$  vs.  $d_0/d$  are shown as an insert.

$[\text{Ru}(\text{bpy})_2\text{L}]^{2+}$ . Therefore, these spectral changes don't arise from the change of solvent polarity or solvent effect, but instead, the hydrogen bonding interaction between the N–H hydrogen in  $[\text{Ru}(\text{bpy})_2\text{L}]^{2+}$  and the N-heterocycle is responsible. Although the complexes,  $[\text{Ru}(\text{bpy})_2(\text{BiImH}_2)]^{2+}$  and  $[\text{Ru}(\text{bpy})_2(\text{BiBzImH}_2)]^{2+}$ , possess two N–H hydrogens, only one-step equilibrium has been observed in the electronic spectra for both complexes

even when the concentration of the N-heterocycle was raised to  $0.05 \text{ mol dm}^{-3}$ . Both N–H bonds in  $\text{BiImH}_2$  or  $\text{BiBzImH}_2$  complexes appear to be too sterically hindered to form two hydrogen bondings at the same time on the  $\text{BiImH}_2$  or  $\text{BiBzImH}_2$  ligand. From the spectral change, the equilibrium constants can be obtained by using eqn. (1); representative linear plots between  $(1 - d_0/d)/[D]$  and  $(d_0/d)$  at two different wavelengths for  $[\text{Ru}(\text{bpy})_2(\text{PBzImH})]^{2+}$  are shown in Fig. 2. Two lines in Fig. 2 cross at the same intercept, which gives us the self-consistent check for the existence of simple equilibrium at each experiment. The equilibrium constants  $K_1$ , which were obtained from the intercepts of the plots, are collected in Table 1. The  $\text{p}K_a$  values of the N-heterocycles are also quoted in Table 1 [15]. The equilibrium constant  $K_1$  was increased with increasing  $\text{p}K_a$  value of the N-heterocycles. When the logarithms of the equilibrium constant,  $\log K_1$ , for  $[\text{Ru}(\text{bpy})_2(\text{PBzImH})]^{2+}$  as a hydrogen donor were plotted against the  $\text{p}K_a$  value of N-heterocycles, a straight line ( $r = 0.958$ ) was obtained (Fig. 3). This linear correlation indicates that the higher basicity on the nitrogen of the N-heterocycle leads to stronger attraction between the N–H bond in the complexes as a hydrogen bonding donor and the N-lone pair on the N-heterocycle as a hydrogen bonding acceptor. On the other hand, the smaller  $\text{p}K_a$  value of the complex results in a larger equilibrium constant  $K_1$  when 4-methylpyridine was fixed as a hydrogen bonding acceptor (Table 2). Consequently, the complex having the more acidic proton makes the hydrogen bonding interaction stronger.

TABLE 1. Equilibrium constants and the magnitude of the oxidation potential shift for the hydrogen bonding interaction of  $[\text{Ru}(\text{bpy})_2\text{L}]^{2+}$  with N-heterocycles at  $25^\circ\text{C}$  in  $\text{CH}_3\text{CN}$

N-heterocycles	$\text{p}K_a$	$K_1^a$ ( $\text{mol}^{-1} \text{ dm}^3$ )	$K_{\text{II}}^b$ ( $\text{mol}^{-1} \text{ dm}^3$ )	$\Delta E^c$ (V)
L = PBzImH				
3-Chloropyridine	2.81	0.26	$6.5 \times 10^2$	0.20
4-Acetylpyridine	3.51	2.90	$7.8 \times 10^4$	0.26
Pyridine	5.23	12.0	$1.2 \times 10^7$	0.36
4-t-Butylpyridine	5.66	81.3	$1.9 \times 10^8$	0.38
4-Methylpyridine	5.98	80.0	$5.0 \times 10^8$	0.40
1-Methylimidazole	6.95	5700	$2.4 \times 10^{11}$	0.45
L = BiBzImH <sub>2</sub>				
3-Chloropyridine	2.81	3.3	$5.5 \times 10^4$	0.25
4-Acetylpyridine	3.51	29.0	$8.4 \times 10^6$	0.32
Pyridine	5.23	53.0	$7.0 \times 10^7$	0.36
4-t-Butylpyridine	5.66	2380	$5.4 \times 10^9$	0.38
4-Methylpyridine	5.98	1900	$7.4 \times 10^9$	0.39

<sup>a</sup>The values were obtained spectrophotometrically.

<sup>b</sup>The values were calculated from the equation  $K_{\text{II}} = K_1 \exp[(F\Delta E)/RT]$ .

<sup>c</sup>The magnitude of the potential shift in oxidation process due to the hydrogen bonding interaction,  $\Delta E = E_{\text{non}} - E_{\text{H-bond}}$ .

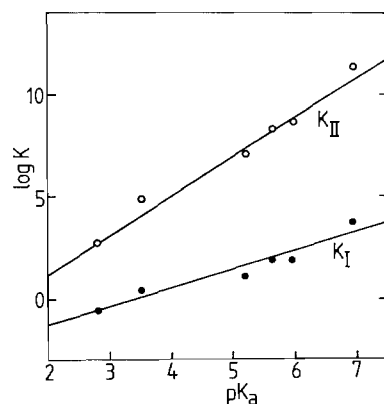


Fig. 3. Plots of  $\log K$  vs.  $pK_a$  of N-heterocycles for  $[\text{Ru}(\text{bpy})_2(\text{PBzImH})]^{n+}$  ( $K_I$  for  $n = 2$  or  $K_{II}$  for  $n = 3$ ).

TABLE 2. Equilibrium constants for the hydrogen bonding interaction of 4-methylpyridine with  $[\text{Ru}(\text{bpy})_2\text{L}]^{2+}$  at 25 °C in  $\text{CH}_3\text{CN}$

L	$pK_a$ value of complex <sup>a</sup>	$K_I^b$ (mol <sup>-1</sup> dm <sup>3</sup> )
PImH	7.9	8.9
BiImH <sub>2</sub>	7.3	10.2
PBzImH	6.8	80.0
BiBzImH <sub>2</sub>	5.7	1900

<sup>a</sup>Data obtained from ref. 12. <sup>b</sup>The values were obtained spectrophotometrically.

#### Effect of Hydrogen Bonding on the Ru(II/III) Oxidation Potential

The variation of the Ru(II/III) oxidation potential on addition of the N-heterocycles has been studied by cyclic voltammetry (Fig. 4). The cyclic voltammogram of  $[\text{Ru}(\text{bpy})_2(\text{PBzImH})]^{2+}$  in  $\text{CH}_3\text{CN}$  shows a chemically reversible Ru(II/III) oxidation wave at +0.77 V versus  $\text{Fc}/\text{Fc}^+$ , as reported previously [12]. Addition of 4-methylimidazole ( $5.3 \times 10^{-5}$  mol dm<sup>-3</sup>) to a solution of  $[\text{Ru}(\text{bpy})_2(\text{PBzImH})]^{2+}$  in  $\text{CH}_3\text{CN}$  resulted in the appearance of an extra new oxidation wave at a more negative potential (Fig. 4b). The new wave was proportional in intensity to the amount of added 4-methylimidazole (Fig. 4c–e). Only the new oxidation couple was finally observed (Fig. 4f). In the case of a weaker base than 4-methylimidazole, a similar behavior was observed, except a larger proportion of N-heterocycles was required to bring about the disappearance of the wave. Furthermore, the potential for the new wave was shifted to the negative direction and approached the constant potential value. The potential difference between initial and final wave,  $\Delta E (= E_{\text{non}} - E_{\text{H-bond}})$ , depends on the base strength

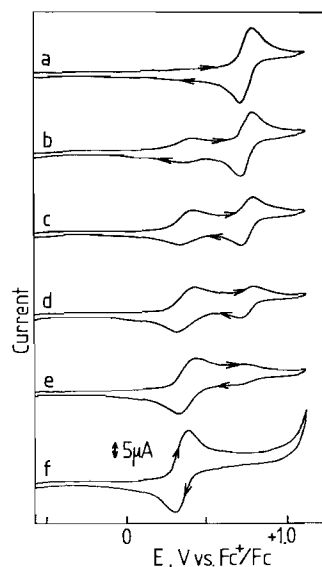


Fig. 4. Cyclic voltammograms for the oxidation of  $4.5 \times 10^{-4}$  mol dm<sup>-3</sup>  $[\text{Ru}(\text{bpy})_2(\text{PBzImH})]^{2+}$  in  $\text{CH}_3\text{CN}$  at a platinum electrode at 25 °C in the absence (a) and in the presence of different concentration of 1-methylimidazole (MeIm) (b–f): [MeIm] = (b)  $5.34 \times 10^{-5}$ , (c)  $1.07 \times 10^{-4}$ , (d)  $1.60 \times 10^{-4}$ , (e)  $2.14 \times 10^{-4}$ , (f)  $3.14 \times 10^{-3}$  mol dm<sup>-3</sup>.

$pK_a$  of the N-heterocycles, where  $E_{\text{non}}$  is the potential in the absence of additives and  $E_{\text{H-bond}}$  is that of the hydrogen bonded complex. A plot of  $\Delta E$  against  $pK_a$  of the added bases is found to be linear as shown in Fig. 5. This result reveals that the electron density on the ruthenium increases indirectly through hydrogen bonding between the N–H bond in the complex and the N-heterocycles. The increase of the electron density on the ruthenium can be qualitatively interpreted by an increase in the proportion of an ionic resonance form B shown in Scheme 1. The increase of electron density on Ru leads to the rise of the  $d\pi$  orbital energy in  $[\text{Ru}(\text{bpy})_2\text{L}]^{2+}$  by the outer-sphere hydrogen bonding perturbation, which is consistent with the negative shift on the oxidation potential and the red shifting of

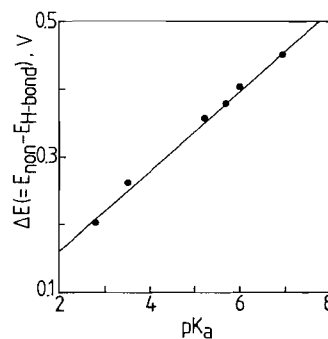
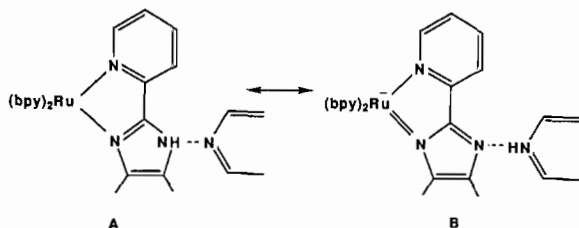


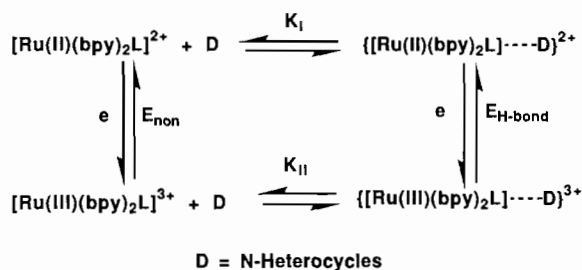
Fig. 5. Plot of the potential difference for  $[\text{Ru}(\text{bpy})_2(\text{PBzImH})]^{2+}$ ,  $\Delta E$ , against  $pK_a$  of N-heterocycles.



Scheme 1.

the metal-to-ligand charge-transfer (MLCT) band around 460 nm. A similar potential shift on the hydrogen bonding has been reported for organic systems, and the relative basicity of the base in the medium has been estimated from the potential shift [16].

Thus, we can suggest that the basicity of the unknown amino acid residue in the polypeptide could be predicted from the amount of the potential shift when the Ru–imidazole or –benzimidazole complexes are used as an electrochemical probe. Further investigations are under way.



Scheme 2.

The thermodynamic cycles in Scheme 2 are now considered. Since the values  $K_I$ ,  $E_{\text{non}}$ , and  $E_{\text{H-bond}}$  have been obtained, and thus the equilibrium constant for the Ru(III) state,  $K_{\text{II}}$  value, will be evaluated by the following equation

$$K_{\text{II}} = K_I \exp \left[ \frac{F\Delta E}{RT} \right] \quad (2)$$

where  $\Delta E$  is  $E_{\text{non}} - E_{\text{H-bond}}$ , and  $F$ ,  $R$  and  $T$  are the Faraday constant, gas constant and temperature, respectively. The calculated  $K_{\text{II}}$  values are collected in Table 1, and a plot of  $\log K_{\text{II}}$  versus the  $\text{p}K_{\text{a}}$  value of the N-heterocycles is also included in Fig. 3. The change in the Ru oxidation state from Ru(II) to Ru(III) results in a dramatic increase in the  $K_{\text{II}}$  value (Table 1). This suggests that the ionic resonance form B in Scheme 2 is more stabilized when the positive charge on the Ru state is increased, and thus the hydrogen bonding interaction for the Ru(III) state becomes much stronger by a factor of about

$10^6$ . Recently, we have reported the  $\text{p}K_{\text{a}}$  value of Ru(II) and Ru(III)–BiBzImH<sub>2</sub> complexes [17], in which the  $\text{p}K_{\text{a}}$  value of the Ru(III) state is much smaller than that of the Ru(II) state. A smaller  $\text{p}K_{\text{a}}$  value of metal–imidazole complexes has also been reported for the complex with the larger metal oxidation state [18]. Thus, the difference in  $\text{p}K_{\text{a}}$  value between the Ru(II) and Ru(III) oxidation states reflects that of the strength of hydrogen bonding for the present system.

In conclusion, the hydrogen bonding interaction of Ru–imidazole and –benzimidazole complexes with N-heterocycles leads to the control of the Ru electronic state by the selection of  $\text{p}K_{\text{a}}$  of the N-heterocycles. On the other hand,  $\Delta E$  will be a measure of the hydrogen bonding interaction and a simple method to know the relative strength of the base. Therefore, Ru–imidazole and –benzimidazole complexes will have potentiality as a spectrophotometric and electrochemical probe for examining the environment in enzymes and related biopolymers [19].

#### Acknowledgement

This work was partially supported by a Grand-in-Aid for Scientific Research, No. 62540461, from the Ministry of Education. We thank Professor M. Masui for helpful discussions.

#### References

- (a) T. G. Traylor, A. Berzinis, D. Campbell, J. Cannon, W. Lee, D. McKinnon, T. Mincey and D. K. White, in W. S. Caughey (ed.), *Oxygen: Biochemical and Clinical Aspects*, Academic Press, New York, 1979, pp. 455–476; (b) J. C. Swartz, M. A. Stanford, J. N. Moy, B. M. Hoffmann and J. S. Valentine, *J. Am. Chem. Soc.*, **101** (1979) 3396–3398; (c) M. A. Stanford, J. C. Swartz, T. E. Phillips and B. M. Hoffmann, *J. Am. Chem. Soc.*, **102** (1980) 4492–4499; (d) T. G. Traylor, *Acc. Chem. Res.*, **14** (1981) 102–109.
- F. A. Walker, M. L. Lo and M. T. Ree, *J. Am. Chem. Soc.*, **98** (1976) 5552.
- P. Stein, M. Mitchell and T. G. Spiro, *J. Am. Chem. Soc.*, **102** (1980) 7795.
- (a) M. M. Doeff, D. A. Sweigart and P. O'Brien, *Inorg. Chem.*, **22** (1983) 851–852; (b) A. L. Balch, J. J. Watkins and D. J. Doonan, *Inorg. Chem.*, **18** (1979) 1228–1231; (c) W. Byers, J. A. Cossham, J. O. Edwards, A. T. Gordon, J. G. Jones, E. T. P. Kenny, A. Mahmood, J. McKnight, D. A. Sweigart, G. A. Tondreau and T. Wright, *Inorg. Chem.*, **25** (1986) 4767–4774.
- (a) T. Taura, *J. Am. Chem. Soc.*, **101** (1979) 4221–4228; (b) U. Sakaguchi, S. Tamaki, K. Tomioka and H. Yoneda, *Inorg. Chem.*, **24** (1985) 1624–1627.
- V. Balzani, N. Sabbatini and F. Scandola, *Chem. Rev.*, **86** (1986) 319–337.
- J. C. Curtis, B. P. Sullivan and T. J. Meyer, *Inorg. Chem.*, **22** (1983) 224–236.
- M. Haga, *Inorg. Chim. Acta*, **77** (1983) L39–41.

- 9 A. Juris, V. Balzani, F. Barigelletti, S. Campagna, P. Belser and A. von Zelewsky, *Coord. Chem. Rev.*, **84** (1988) 85–277, and refs. therein.
- 10 E. Barni and P. Savarino, *J. Heterocyclic Chem.*, **14** (1977) 937.
- 11 D. T. Sawyer and J. L. Roberts, Jr., *Experimental Electrochemistry for Chemists*, Wiley, New York, 1974, p. 212.
- 12 M. Haga, *Inorg. Chim. Acta*, **75** (1983) 29.
- 13 R. R. Gagne, C. A. Koval and G. C. Lisensky, *Inorg. Chem.*, **19** (1980) 2854.
- 14 N. Mataga and S. Tsuno, *Bull. Chem. Soc. Jpn.*, **30** (1957) 368–374.
- 15 R. C. Weast, M. J. Astle and W. H. Beyer (eds.), *CRC Handbook of Chemistry and Physics*, CRC Press, Boca Raton, 69th edn., 1988, p. D-159.
- 16 (a) M. Masui, Y. Kaiho and S. Ozaki, *Chem. Pharm. Bull.*, **29** (1981) 1772–1774; (b) M. Masui, Y. Kaiho, T. Ueshima and S. Ozaki, *Chem. Phar. Bull.*, **30** (1982) 3225–3230.
- 17 A. M. Bond and M. Haga, *Inorg. Chem.*, **25** (1986) 4507.
- 18 M. F. Hoq and R. E. Shepherd, *Inorg. Chem.*, **23** (1984) 1851–1858.
- 19 J. K. Barton, J. M. Goldberg, C. V. Kumar and N. J. Turro, *J. Am. Chem. Soc.*, **108** (1986) 2081.